Manipulating Single Enzymes by an External Harmonic Force

Michael A. Lomholt,[1] Michael Urbakh,[2] Ralf Metzler,[1,3] and Joseph Klafter[2]

[1]*Physics Department, University of Ottawa, 150 Louis Pasteur, Ottawa, ON, K1N 6N5, Canada*
[2]*School of Chemistry, Tel Aviv University, 69978 Tel Aviv, Israel*
[3]*NORDITA, Blegdamsvej 17, DK-2100 Copenhagen Ø, Denmark*

(Received 1 November 2006; published 19 April 2007)

We study a Michaelis-Menten reaction for a single two-state enzyme molecule, whose transition rates between the two conformations are modulated by an harmonically oscillating external force. In particular, we obtain a range of optimal driving frequencies for changing the conformation of the enzyme, thereby controlling the enzymatic activity (i.e., product formation). This analysis demonstrates that it is, in principle, possible to obtain information about particular rates within the kinetic scheme.

DOI: 10.1103/PhysRevLett.98.168302 PACS numbers: 82.37.−j, 02.50.Ey, 82.20.Fd, 87.64.Dz

Recent advances in single molecule spectroscopy have made it possible to follow the catalytic activity of individual enzymes over extended periods of time [1–6]. Although the catalytic rates have been shown to be distributed in time, the general Michaelis-Menten scheme, originally proposed for an ensemble of enzymes, turned out to hold quite well also on the level of a single enzyme [1–8]. What is still left open is the nature of the conformational changes and its relationship to the enzymatic activity [6–9]. Deeper insights into the conformational-activity relationship can be obtained by influencing single enzyme conformations by an external force and following the effects on the catalytic activity. The possibility to manipulate enzymatic turnovers by applying a mechanical force has been recently demonstrated in Ref. [10]. Also, voltage-gated ion channels can be manipulated electrically to switch between two states [11]. Here, assuming a two-state Michaelis-Menten scheme for a single enzyme, we investigate how one can manipulate the activity (turnovers) of an enzyme by an external harmonic force. The oscillatory force is shown to be able to increase the weight (occurrence time) of a desired conformation in the scheme, controlling the enzyme activity.

The reaction scheme that we examine is shown in Fig. 1. We model the effect of the time-dependent external force as a shift in the conformational energy landscape. Assuming that the transitions between different conformations, with rates α_{ij} and β_{ij}, follow an Arrhenius activation, and using a harmonic force which modulates barriers separating conformational states, we find the following time dependence of the rates:

$$\alpha_{ij} = \alpha_{ij}(t) = \alpha_{ij}^{(0)} \exp[-\epsilon_{ij}^{(\alpha)} \sin(\omega t + \phi_0)], \quad (1a)$$

$$\beta_{ij} = \beta_{ij}(t) = \beta_{ij}^{(0)} \exp[-\epsilon_{ij}^{(\beta)} \sin(\omega t + \phi_0)]. \quad (1b)$$

Here ω is the angular frequency of the external driving force, ϕ_0 is the initial phase of the force, and $\alpha_{ij}^{(0)}$, $\beta_{ij}^{(0)}$, $\epsilon_{ij}^{(\alpha)}$, and $\epsilon_{ij}^{(\beta)}$ are phenomenological constants characterizing the enzyme and the amplitude of the driving force. In Eqs. (1), we assume that the potential energy landscape of the conformations responds instantly to changes in the force. This assumption can be relaxed, for instance, by including different phases ϕ_0 for α_{ij} and β_{ij}. Note, however, that a 180° phase difference, corresponding to a change of sign for $\epsilon_{ij}^{(\beta)}$, is included in Eqs. (1). We assume that the substrate S is in great excess, such that the rates for the reaction with the substrate like $k_{1i} = k_{1i}^{(0)}[\mathrm{S}]$ become independent of time. The scheme in Fig. 1 is closely related to schemes describing resonant activation in discrete systems [12].

Simulations.—As shown below, for certain limits of the rates, analytical expressions can be derived. To obtain insight into the general behavior of enzymatic activity including noise, we use a stochastic simulation. To this end, we implemented the Gillespie algorithm [13], which provides random values for the waiting time between two reaction steps and the direction of the reaction as weighted by the corresponding Arrhenius factor. We start the system in one of the states $\mathrm{E}_i + \mathrm{S}$ and then perform jumps to one of the neighboring states according to the Gillespie reaction probability. To which state it jumps is decided by picking a waiting time for jumping to state ES_i according to the exponential distribution with rate parameter k_{1i} and one for jumping to $\mathrm{E}_j + \mathrm{S}$ according to the cumulative distribution

$$F_{\alpha_{ij}}(\Delta t) = 1 - \exp\left(-\int_t^{t+\Delta t} \alpha_{ij}(t')dt'\right), \quad (2)$$

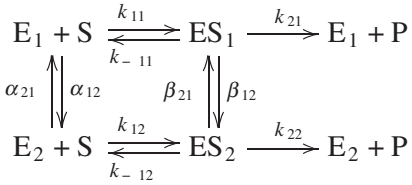

FIG. 1. Michaelis-Menten scheme for a single enzyme with two conformations. E denotes the enzyme molecule, S the substrate, and P the product. Rates α_{ij} and β_{ij} $(i, j = 1, 2)$ stand for transitions between conformational states 1 and 2, while rates k_{xi} $(x = -1, 1, 2)$ quantify internal conversions.

and then the jump is made to the state with the shortest waiting time. Subsequent jumps to neighboring states are determined similarly, and one iteration of the simulation stops at time $t = \tau$ when the system reaches one of the product states $E_i + P$. The conformation i of the enzyme is then used as the initial state for the next iteration with the initial phase $\phi_0^{(\mathrm{new})} = \omega\tau + \phi_0^{(\mathrm{old})}$ determining the new momentary force. By performing iterations over many periods of the oscillating force, we obtain a time series for the turnover times τ, from which the average waiting time $\langle\tau\rangle$ yields. Plots of $\langle\tau\rangle$ as a function of ω are shown in Figs. 2 and 6. Depending on the choice of parameters, switching between two or three kinetic regimes of the system is revealed. Certain limiting behaviors are accessible analytically, as discussed soon. For the parameters used throughout this work, the rate of product formation in conformation 2 is higher than in conformation 1.

We note that in our analysis the parameters [except for case (ii) in Fig. 2] are chosen such that detailed balance is fulfilled, as required for certain single enzymes that are coupled to the surrounding heat bath [14]. The explicit condition arising when detailed balance is applied around the loop in the reversible reaction pathway in Fig. 1 is $k_{-11}\beta_{21}(t)k_{12}\alpha_{12}(t) = k_{11}\beta_{12}(t)k_{-12}\alpha_{21}(t)$. The condition is applied for any momentary value of the external force, and therefore any time t, since the system could equally well be held constantly at these forces. Detailed balance could be violated, for instance, by enzymes converting ATP energy during their cycle.

Fast switching limit.—Consider the case when the switching between enzyme conformations is much faster than the reactions with the substrate, as displayed in Fig. 2. Note that case (ii) in Fig. 2 has different k_{1i}'s [15]. It also

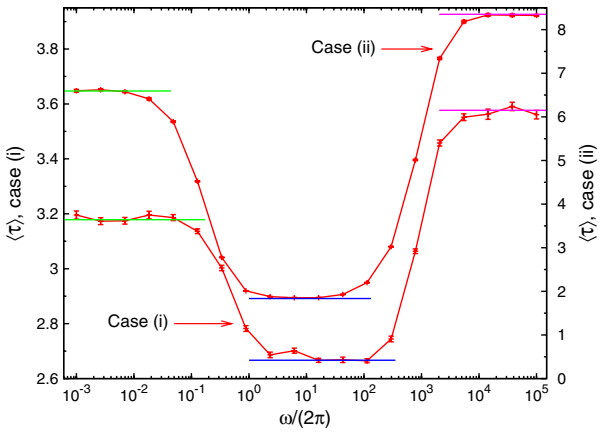

FIG. 2 (color online). Mean turnover time $\langle\tau\rangle$ as a function of driving frequency ω for the case $k_{xi} \ll \alpha_{ij}, \beta_{ij}$. Horizontal lines represent the limit cases derived in the text. (i) $k_{1i} = k_{-1i} = 1$, $k_{21} = 0.3$, $k_{22} = 3$, $\alpha_{12}^{(0)} = 80$, $\alpha_{21}^{(0)} = 800$, $\beta_{12}^{(0)} = 160$, $\beta_{21}^{(0)} = 1600$, $\epsilon_{12}^{(\alpha)} = 2 = -\epsilon_{21}^{(\beta)}$, $\epsilon_{12}^{(\beta)} = 3 = -\epsilon_{21}^{(\alpha)}$. (ii) The following parameters were changed: $k_{11} = k_{-11} = k_{-12} = 0.01$, $k_{12} = 3 = -\epsilon_{12}^{(\beta)}$, $\epsilon_{21}^{(\beta)} = 2$ (units on the right axis). Simulations were run for 5×10^4 turnovers per frequency.

includes a 180° shift in the phases of variation of rates α_{ij} and β_{ij} under the external force distinguishing between substrate-bound and substrate-free enzyme states. Parameters were chosen to reflect situations with enhanced enzyme efficiency at intermediate frequencies. Different scenarios, for instance, with decreased efficiency, are also possible. In both cases in Fig. 2, the rates satisfy $k_{xi} \ll \alpha_{ij}, \beta_{ij}$. This means that we can define effective rates k_x as averages over the various conformations. The weights in these averages are given by the probabilities for the enzyme to be in the different conformations. If ω is much faster or slower than the relaxation time between the two enzyme conformations, these probabilities can be easily obtained. For instance, the probability for the enzyme to be in conformation E_1, given that no substrate is bound, is

$$p(1|\mathrm{E}, \phi) = \begin{cases} \alpha_{21}(\phi)/[\alpha_{12}(\phi) + \alpha_{21}(\phi)], & \omega \ll \alpha_{ij}, \\ \bar{\alpha}_{21}/[\bar{\alpha}_{12} + \bar{\alpha}_{21}], & \omega \gg \alpha_{ij}, \end{cases} \tag{3}$$

where $\phi \in (0, 2\pi)$ is the phase of the force, i.e., $\omega t + \phi_0 = \phi + 2\pi n$ for some integer n, and a bar over a quantity means that this quantity is averaged over all phases:

$$\bar{\alpha}_{ij} = \int_0^{2\pi} \frac{d\phi}{2\pi} \alpha_{ij}(\phi) = \alpha_{ij}^{(0)} I_0(\epsilon_{ij}^{(\alpha)}), \tag{4}$$

where I_0 is the modified Bessel function of order 0. The effective rates k_x can now be obtained in the two limits:

$$k_x(\phi) = \begin{cases} \sum_i k_{xi} p(i|x, \phi), & \omega \ll k_{xi}, \\ \sum_i k_{xi} \bar{p}(i|x), & \omega \gg k_{xi}, \end{cases} \tag{5}$$

where x in $p(i|x, \phi)$ refers to the unbound state E + S for $x = 1$ and to the bound state ES for $x = -1$ and $x = 2$. The rate of the overall reaction is then given by the standard Michaelis-Menten expression [3,4,14]

$$\nu(\phi) = \frac{k_2(\phi)k_1(\phi)}{k_1(\phi) + k_{-1}(\phi) + k_2(\phi)} \tag{6}$$

as a function of the phase ϕ. The average waiting time $\langle\tau\rangle$ for one turnover can now be found by averaging over all phases and calculating $\langle\tau\rangle = 1/\bar{\nu}$. The values of $\langle\tau\rangle$ calculated according to Eqs. (5) and (6) are shown in Fig. 2 by the horizontal lines. We note that the limits where $\omega \ll \alpha_{ij}, \beta_{ij}$ can also be obtained as limit cases of the system studied in Ref. [16].

Another experimentally relevant quantity is the temporal probability density for the formation of products at a given value of the force as determined by the phase ϕ. A plot of this intensity of product formation events, which we label by $\langle I(\phi)\rangle$, is shown in Fig. 3. An approximate bimodal behavior is found for certain choices of the parameters. To obtain the analytic limits, we note that if the external force is slowly varying, i.e., $\omega \ll k_{xi}, \alpha_{ij}, \beta_{ij}$, then the intensity will simply be equal to the rate $\langle I(\phi)\rangle = \nu(\phi)$. This ex-

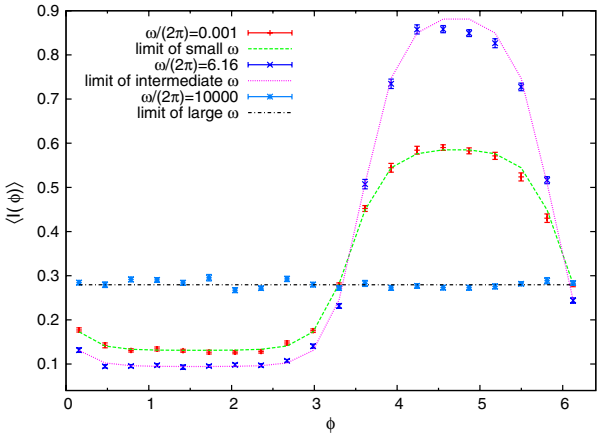

FIG. 3 (color online). Plot of $\langle I(\phi)\rangle$ as a function of ϕ for different driving frequencies ω, for the same conditions as in Fig. 2(i).

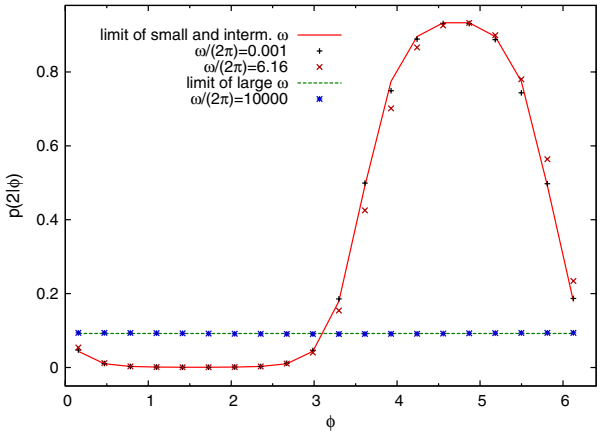

FIG. 4 (color online). Estimate of $p(2|\phi)$ as a function of ϕ for the same parameters as in Fig. 2(i). Note that there are only two different analytic limits, since two of the three limits are identical for the chosen parameters.

pression also holds for $\omega \gg \alpha_{ij}, \beta_{ij}$, where it is independent of ϕ. For the intermediate ω where $k_{xi} \ll \omega \ll \alpha_{ij}, \beta_{ij}$, it will be the distribution of conformations in the final step of the reaction and the corresponding rate constants that determine when the product formation happens, such that $\langle I(\phi)\rangle = \bar{\nu}\sum_i k_{2i} p(i|\mathrm{ES}, \phi)/\bar{k}_2$. We point out here that at slow frequencies it is the overall efficiency of the enzyme that is probed at different magnitudes of the external force, while at the intermediate frequencies it is only the relative efficiency of the final step in the reaction which is probed at different external driving. Thus, tuning the frequency allows one to selectively study the final reaction step.

The behavior of $\langle I(\phi)\rangle$ in Fig. 3 can be compared with the probability of being in, say, conformation 2 (the fast one) as a function of ϕ, as shown in Fig. 4. Note the large change in amplitude for the chosen parameters. To obtain the analytic limits, we write the probability as $p(i|\phi) = p(i|\mathrm{E}, \phi)p(\mathrm{E}|\phi) + p(i|\mathrm{ES}, \phi)[1 - p(\mathrm{E}|\phi)]$, where $p(i|\mathrm{E}, \phi)$ is given by Eq. (3). To find $p(E|\phi)$, note that at a given phase ϕ the effective rate for the system to leave the state without a bound substrate is $k_1(\phi)$, and the rate for leaving the state with bound substrate is $k_{-1}(\phi) + k_2(\phi)$. In fact, the quasi-steady-state probability for being in the state without a bound substrate is

$$p(\mathrm{E}|\phi) = \frac{k_{-1}(\phi) + k_2(\phi)}{k_1(\phi) + k_{-1}(\phi) + k_2(\phi)} \tag{7}$$

in the two cases given by Eq. (5) where either $\omega \ll k_{xi}$ or $\omega \gg k_{xi}$. The resemblance of Figs. 3 and 4 reflects the dominating role of conformation 2, due to its larger catalytic rate, in the enzymatic activity.

To illustrate further the mechanisms behind the transitions of $\langle\tau\rangle$ with changing driving frequency, we plotted the fraction of time the enzyme spends in conformation 2, labeled $p(2)$, during a simulation run in Fig. 5. The analytic limits of $p(2)$ can be obtained straightforwardly by averaging the probability of being in conformation 2 over all phases $p(i) = \int_0^{2\pi}[d\phi/(2\pi)]p(i|\phi)$. This behavior can be compared with the fraction of product formation events that occurs while the enzyme is in conformation 2, labeled by $p(2|\mathrm{E} + \mathrm{P})$ in Fig. 5. The analytical limits of $p(2|\mathrm{E} + \mathrm{P})$ can be obtained by averaging over all phases ϕ the effective rate constant for forming a product in conformation i, $k_{2i}p(i|\mathrm{ES}, \phi)$, divided by the overall effective $k_2(\phi)$, taking into account the varying rate of product formation by a factor $\nu(\phi)/\bar{\nu}$. The explicit formula is

$$p(i|\mathrm{E} + \mathrm{P}) = \int_0^{2\pi} \frac{d\phi}{2\pi} \frac{k_{2i}p(i|\mathrm{ES}, \phi)}{k_2(\phi)} \frac{\nu(\phi)}{\bar{\nu}}. \tag{8}$$

As Fig. 5 illustrates, the slowing down of the reaction with increasing frequency at the second transition in Fig. 2 occurs because the high frequency of the force shifts the enzyme towards spending more time in the low efficiency conformation. The increased efficiency of the enzyme at

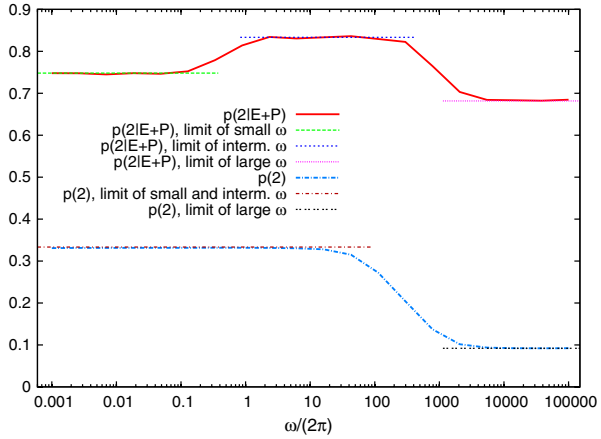

FIG. 5 (color online). Plot of the fraction $p(2)$ the enzyme spends in conformation 2 (lower curve), as a function of driving frequency ω for the same parameters used in Fig. 2(i). The upper curve depicts the fraction of product formation while the enzyme is in conformation 2.

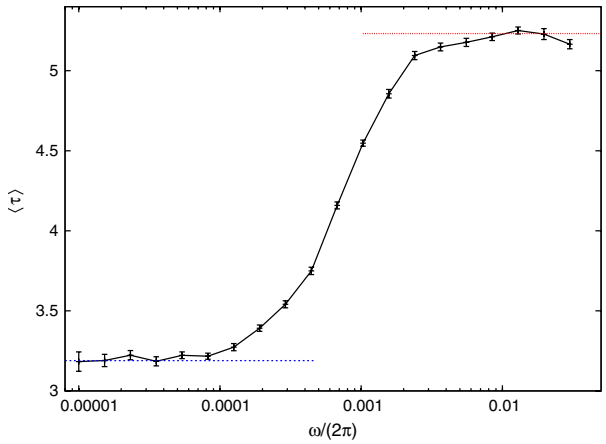

FIG. 6 (color online). Plot of $\langle\tau\rangle$ as function of driving frequency ω for $\alpha_{ij}, \beta_{ij} \ll k_{xi}$. The horizontal lines represent the limits derived in the text. The parameters are $k_{1i} = k_{-1i} = 1$, $k_{21} = 0.3$, $k_{22} = 3$, $\alpha_{12}^{(0)} = 2 \times 10^{-4}$, $\alpha_{21}^{(0)} = 10^{-3}$, $\beta_{12}^{(0)} = 2 \times 10^{-5}$, $\beta_{21}^{(0)} = 10^{-4}$, $\epsilon_{12}^{(\alpha)} = 3$, $\epsilon_{21}^{(\alpha)} = -3$, $\epsilon_{12}^{(\beta)} = 3$, and $\epsilon_{21}^{(\beta)} = -3$. The simulation comprises 2×10^6 turnovers per frequency.

intermediate frequencies sets in when the external force drives the enzyme back and forth between its two conformations fast enough to avoid the bottleneck of the enzyme spending long uninterrupted periods being forced towards the slowly reacting conformation.

Slow switching limit.—When the switching between enzyme states is slow in comparison to substrate reactions, $\alpha_{ij}, \beta_{ij} \ll k_{xi}$, the enzyme will mostly stay in the same state during a reaction cycle, and we can therefore take the instantaneous reaction rate to be

$$\nu(\phi) = p(1|\phi)\nu_1 + p(2|\phi)\nu_2, \tag{9}$$

where $\nu_i = k_{2i}k_{1i}/(k_{1i} + k_{-1i} + k_{2i})$ are the fixed conformation rates, and $p(i|\phi)$ is the probability for the enzyme to be in conformation i at a given phase of the oscillating force. To find this probability, we first argue in the same way as Eq. (7) was obtained to see that the (steady-state) probability of being in the state without a bound substrate, given that the conformation is i, is

$$p(\mathrm{E}|i) = \frac{k_{-1i} + k_{2i}}{k_{1i} + k_{-1i} + k_{2i}}. \tag{10}$$

Then we note that the effective rate constant for changing conformation from i to j can be found as

$$\gamma_{ij} = p(\mathrm{E}|i)\alpha_{ij} + [1 - p(\mathrm{E}|i)]\beta_{ij}. \tag{11}$$

This effective rate now allows the probability of being in conformation i to be calculated similarly to Eq. (3) as

$$p(i|\phi) = \begin{cases} \gamma_{ji}(\phi)/[\gamma_{ij}(\phi) + \gamma_{ji}(\phi)], & \omega \ll \gamma_{ij}, \\ \bar{\gamma}_{ji}/[\bar{\gamma}_{ij} + \bar{\gamma}_{ji}], & \omega \gg \gamma_{ij}, \end{cases} \tag{12}$$

where $j = 3 - i$. The averaged waiting time for one turnover can again be found as $\langle\tau\rangle = 1/\bar{\nu}$.

Discussion.—Detailed knowledge of the dynamics of single enzymes as well as their response to external stimulus is important for the understanding of biochemical processes occurring in living cells. We studied the response of a single two-state enzyme to a harmonic external driving force in the presence of thermal noise. By combination of analytic and simulations results, we demonstrated the rich response behavior of the turnover dynamics of the enzyme to an external force. We showed that in some cases there exist optimum driving frequencies that minimize the turnover time of the enzyme. In these cases, one can selectively obtain information on the reaction rates in the final step of the Michaelis-Menten reaction by choosing an oscillation in a suitable frequency range. Moreover, we found that the response of the enzyme activity can be very sensitive within a small range of phase ϕ, a signature of many biological switches. We note that it should be possible to access the full spectrum of relevant driving frequencies by combining different experimental methods, such as atomic force microscopy and optical switching methods.

M. A. L. and R. M. acknowledge partial funding from the Natural Sciences and Engineering Research Council (NSERC) of Canada and the Canada Research Chairs program. M. U. and J. K. acknowledge financial support from the Deutsche Forschungsgemeinschaft (HA 1517/26-1,2 single molecules).

[1] G. K. Schenter, H. P. Lu, and X. S. Xie, J. Phys. Chem. A **103**, 10 477 (1999).
[2] L. Edman and R. Rigler, Proc. Natl. Acad. Sci. U.S.A. **97**, 8266 (2000).
[3] B. P. English *et al.*, Nat. Chem. Biol. **2**, 87 (2006).
[4] S. C. Kou *et al.*, J. Phys. Chem. B **109**, 19 068 (2005).
[5] O. Flomenbom *et al.*, Proc. Natl. Acad. Sci. U.S.A. **102**, 2368 (2005).
[6] H. P. Lerch, R. Rigler, and A. S. Mikhailov, Proc. Natl. Acad. Sci. U.S.A. **102**, 10 807 (2005).
[7] W. Min *et al.*, J. Phys. Chem. B **110**, 20 093 (2006).
[8] X. Xue, F. Liu, and Zh. Ou-Yang, Phys. Rev. E **74**, 030902(R) (2006).
[9] O. Flomenbom and R. J. Silbey, Proc. Natl. Acad. Sci. U.S.A. **103**, 10 907 (2006).
[10] V. A. P. Wiita *et al.*, Proc. Natl. Acad. Sci. U.S.A. **103**, 7222 (2006).
[11] M. A. Pustovoit, A. M. Berezhkovskii, and S. M. Bezrukov, J. Chem. Phys. **125**, 194907 (2006).
[12] O. Flomenbom and J. Klafter, Phys. Rev. E **69**, 051109 (2004).
[13] D. T. Gillespie, J. Comput. Phys. **22**, 403 (1976).
[14] I. V. Gopich and A. Szabo, J. Chem. Phys. **124**, 154712 (2006).
[15] In case (i) of Fig. 2, we kept $k_{12} = k_{11}$ in accordance with the experimental data [3], which indicate a difference between the values of k_{2i} only.
[16] R. D. Astumian and B. Robertson, J. Am. Chem. Soc. **115**, 11063 (1993).